HIGH-THROUGHPUT IONIC LIQUID ELECTROSPRAY SOURCES BASED ON DENSE MONOLITHIC ARRAYS OF EMITTERS WITH INTEGRATED EXTRACTOR GRID AND CARBON NANOTUBE FLOW CONTROL STRUCTURES

F.A. Hill, P. J. Ponce de Leon, and L.F. Velásquez-García
Massachusetts Institute of Technology, Cambridge, MA, United States

ABSTRACT

We report the design, fabrication, and experimental characterization of externally-fed, batch-microfabricated electrospray emitter arrays with integrated extractor grid and carbon nanotube flow control structures for low-voltage and high-throughput electrospray of the ionic liquid EMI-BF_4 in vacuum. The conformal carbon nanotube forest on the emitters provides a highly effective wicking structure to transport liquid up the emitter surface to the emission site at the tips. Arrays containing as many as 81 emitters in 1 cm^2 were tested and emission currents as high as 5 μA per emitter in both polarities were measured, with a start-up bias voltage as low as 520 V. Imprints formed on the collector electrode and per-emitter IV characteristics showed excellent emission uniformity.

KEYWORDS

Electrospray, emitter array, ionic liquid, carbon nanotubes, wetting, microfabrication, MEMS

INTRODUCTION

Efficient high-throughput generation of ions using electrospray ionization is of great interest for a number of emerging technological applications including mass-efficient nanosatellite electric propulsion, multiplexed focused ion beam imaging, and high-throughput nanomanufacturing. The current and mass flow rate produced by a single electrospray emitter are relatively small; therefore, arrays of emitters that operate in parallel have been proposed and demonstrated to greatly increase the throughput of the electrospray source [1-3]. In addition to multiplexing, electrospray emitter scaling-down provides several advantages, including (i) sharper emitter tips that operate at lower bias voltages, (ii) miniaturized emitters that can be densely packed into arrays to obtain a large numbers of emission sites per unit area, and (iii) small-scale emitter arrays that can be batch-fabricated at low cost using microfabrication processes.

The current design builds upon previous work on microfabricated electrospray emitter arrays for ionic liquids done by our group [3, 4] by implementing a batch-microfabricated MEMS multiplexed externally-fed electrospray array with integrated extractor grid and carbon nanotube (CNT) flow control structures for high-throughput generation of ions from ionic liquids in vacuum. The design features a hierarchical structure that brings together optimized structures with associated characteristic lengths that span five orders of magnitude: mesoscale deflection springs for precision assembly of an extractor electrode die to an emitter array die to attain low beam interception, micro-sharp emitter tips for low-voltage electrospray emission, and a nanostructured conformal CNT wicking structure that controls the flow rate fed to each emitter to attain high emitter current while maintaining good array emission uniformity.

The emitter die and extractor die are fabricated separately, and are assembled together using deflection springs [5, 6] that clamp onto dowel pins and provide precise alignment of the two components. The electrode separation distance is tuned using insulating spacers. In general, this distance should be small for a low start-up voltage, which is given by [7]

$$V_{start} = \sqrt{\frac{\gamma \cdot R}{\varepsilon_o}} ln\left[\frac{2G}{R}\right] \quad (1)$$

where γ is the surface tension, R is the emitter tip radius, ε_o is the permittivity of free space, and G is the distance from the emitter tip to the edge of the extractor aperture. After operation, the two electrodes are easily disassembled, cleaned and replenished with liquid.

Internally-fed emitters supply liquid to the emission site through a capillary channel; this implementation is not ideal for ion emission because capillary channels typically provide low hydraulic impedance and internally-fed emitters can be prone to clogging, which causes device failure. The implemented electrospray emitters are instead externally-fed, with a dense plasma-enhanced chemical vapor deposited (PECVD) CNT forest conformally grown on the surface of the emitters. The CNT forest acts as a wicking material to transport the ionic liquid from the base of the emitters to the emitter tips where it is ionized due to the strong electric fields present there. The ionic liquid tested in this work, i.e., EMI-BF_4, does not spread on the surface of an uncoated silicon emitter array (the contact angle of EMI-BF_4 on silicon is 38°). However, EMI-BF_4 is found to be highly wetting on a CNT-coated silicon emitter surface, and a drop of EMI-BF_4 spontaneously spreads across the emitter array, impregnating the surface and coating the emitter tips.

In addition to its useful wetting properties, a CNT forest provides hydraulic impedance to the ionic liquid as it flows up the surface of the emitters. Electrospray emission can occur in the ionic regime rather than a mixed ionic/droplet regime if the flow rate to the emission site is sufficiently low [8]. A porous medium can limit the flow across the emitter surface in order to match the low flow rate for ionic emission. CNT films are particularly useful because their porosity, determined by CNT diameter and packing density, is highly tunable by changing the growth parameters. The flow rate in the ionic regime is related to the measured current I by

$$Q = \frac{I\langle M \rangle}{N\, e\, \rho} \quad (2)$$

where $\langle M \rangle$ is the average molar mass of the emitted particles, N is Avogadro's number, e is the elementary

charge and ρ is the density of the liquid; for EMI-BF_4 ($\langle M \rangle$ ~0.2 kg/mol, ρ=1300 kg/m^3), ~5 μA of current per emitter corresponds to Q=8×10^{-15} m^3/s. Flow through a porous medium is governed by Darcy's law

$$\overrightarrow{q_s} = -\frac{K_{ps}}{\mu}\nabla P \qquad (3)$$

where $\overrightarrow{q_s}$ is the volumetric flow rate per unit area, ∇P is the fluid pressure gradient from the base to the tip of the emitter, K_{ps} is the permeability of the medium, and μ is the fluid viscosity. The CNT film is modeled as an array of pillars in order to calculate its permeability, which is a function of the CNT diameter distribution and the packing density. The CNT growth conditions have been tuned to obtain a permeability of ~10^{-13} m^2, which provides sufficient impedance for the flow rate to meet the conditions for the ionic regime.

DESIGN

The electrospray source is composed of two dies, i.e., an emitter die and an extractor grid die (Fig. 1); each die is 2.4 cm by 2.4 cm and 1 mm thick. The emitter dies contain arrays of 4, 9, 25, 49 or 81 emitters in 1 cm^2. The emitters are 300-350 μm tall. The extractor grid die contains a matching array of 500 μm diameter circular apertures that are 250 μm thick. Both dies contain four deflection springs that clamp onto dowel pins to enable precision alignment of the two components [6]. When the two dies are assembled (Fig. 2a), each emitter tip sits precisely underneath a grid aperture (Fig. 2b). Four thin polyimide spacers electrically insulate the two dies and set the emitter-to-extractor separation distance.

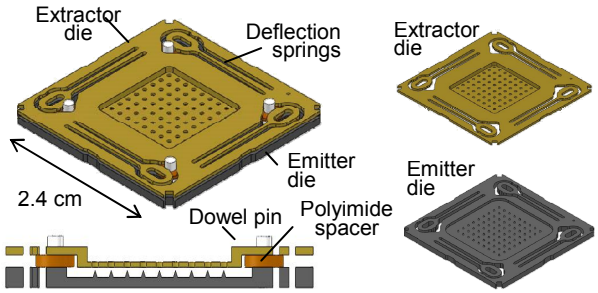

Figure 1: Schematic of the extractor grid die, the emitter die, and their assembly into an electrospray diode using dowel pins and insulating spacers.

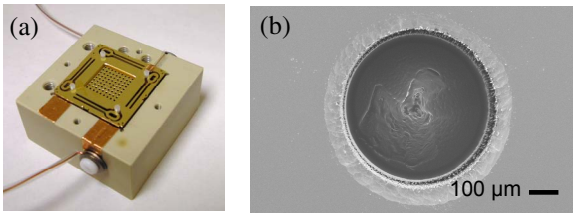

Figure 2: (a) Assembled emitter and extractor electrodes and (b) a SEM image showing alignment of an emitter tip and an extractor aperture.

FABRICATION

The extractor grid and emitter dies (Fig. 3) are fabricated using contact lithography starting with 1 mm thick, double-side polished, doped silicon wafers. The extractor grid dies are fabricated using two deep reactive-ion etching (DRIE) steps. First, the springs and a 750 μm-deep recess for the apertures are etched on the front side of the wafer; then, a second back side DRIE step creates 600 μm-deep recesses around the springs and etches the arrays of apertures. A thin film of titanium/gold is sputtered onto the grid dies to increase their electrical conductivity.

The emitter dies are fabricated by first etching the array of emitter tips on the front side of the wafer using isotropic SF_6 reactive-ion etching (RIE). The masking material is an array of three-notched dots, 292 μm in diameter, patterned in photoresist. The silicon underneath the notched dots is gradually undercut until sharp tips form. Next, a DRIE step etches the springs on the back side of the wafer. To complete the emitter dies, a CNT film is grown on the surface of the emitters. Titanium nitride and nickel films are sputtered onto the 1 cm by 1 cm active area of the emitters using a shadow mask. CNTs are grown using the plasma-enhanced chemical vapor deposition (PECVD) technique with ammonia and acetylene as precursors. The CNTs are 2 μm tall, average 115 nm in diameter, and they conformally coat the surface of the emitters and the entire active area of the emitter dies, as shown in Fig. 4. The PECVD process ensures that the CNTs are firmly attached to the surface of the emitters [9]; no detachment was observed after application of the ionic liquid or after repeated cleaning and reassembly of the electrospray sources.

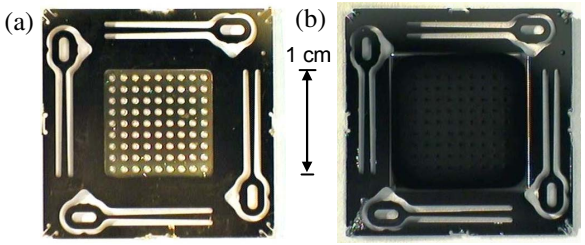

Figure 3: (a) Extractor grid and (b) emitter dies for an array of 81 electrospray emitters in 1 cm^2.

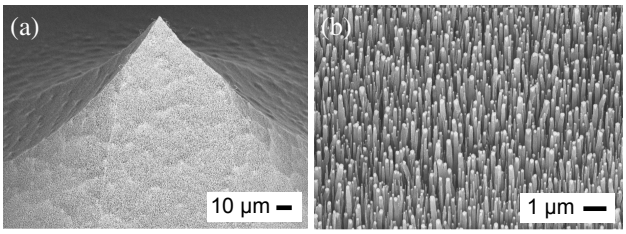

Figure 4: (a) Electrospray emitter and (b) close-up of the CNTs on the emitter surface.

EXPERIMENTAL SETUP

The electrospray sources were tested in a vacuum chamber at a pressure in the 10^{-6} Torr range. For each test, a 0.5 μL drop of EMI-BF_4 was deposited on the surface of the emitters, which spreads spontaneously to coat the surface of the emitter arrays. The liquid stops spreading once it reaches the outer edge of the CNT coated emitter active area and does not wet the

surrounding silicon, thereby avoiding a potential electrical short due to liquid bridges forming between the electrodes at the dowel pins. The emitter and extractor dies are assembled together by clamping the deflection springs onto four acetal dowel pins, with polyimide spacers separating the two electrodes. We used a triode configuration to characterize the performance of the electrospray sources, where a silicon collector electrode, placed 3.5 mm from the emitter die, is used to measure the emission current and also to collect imprints of the emission. The circuit used to test the devices is shown in Fig. 5. A Bertan 225-10R source-measure unit (SMU) was used to bias the emitter electrode up to ±2000 V, alternating the polarity to avoid a build-up of ions of either polarity [10]. A Keithley 6485 picoammeter measures the current intercepted by the extractor grid, and a Keithley 237 SMU was used to measure the collector current. A pair of diodes and a fuse protect the picoammeter from current surges. The extractor electrode was held at 0 V and the collector electrode was biased up to 1000 V with opposite polarity to the polarity of the emitted beam (e.g., a positively biased emitter die would face a negatively biased collector). Data were collected using a PC and a LabView script.

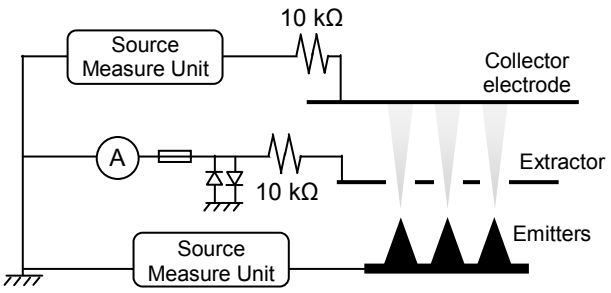

Figure 5: Schematic of the electrospray testing circuit.

RESULTS AND DISCUSSION

The performance of the electrospray sources with different array sizes has been characterized. Across all devices, three different phases of emission are observed: an initial overwet phase, a steady phase, and a depletion phase. Similar behavior was exhibited by our previous generation of surface-fed emitters that use black silicon as wicking material [4]. With fresh liquid applied to the emitter surface, emission is initially noisy and unstable, punctuated by current surges that are thought to be due to droplet emission. Subsequently, emission steadies and is marked by output current as high as 5 µA per emitter. After more than five minutes of operation, the liquid on the surface of the emitters begins to deplete, and beyond a certain bias voltage the current stops increasing. Once the liquid is replenished, the devices can be reused.

The current-voltage characteristics of a 7 by 7 emitter array during the steady emission phase are shown in Fig. 6, with 600 µm (G=320 µm) and 360 µm (G=250 µm) separation between the emitter and extractor electrodes. Thinner spacers 240 µm thick were also tested but these led to liquid shorts forming between the emitter and extractor electrodes shortly after emission began. The curves show a strong non-linear dependence between the current and the bias voltage. The emission current increases exponentially for current below 0.5 µA, and then increases more or less linearly with a slope of 90 nA/V. Considering as start-up voltage the voltage at which the collector current per emitter reaches 5×10^{-6} µA, the start-up voltage is 520 V for the 360 µm spacers and 1200 V for 600 µm spacers. It is clear that reducing the gap between electrodes reduces the operating voltage.

For currents above 50 nA per emitter, the devices typically have ~80% transmission in both polarities. The extractor and emitter current for a 9 by 9 emitter array are plotted in Fig. 7, showing an intercepted current on the extractor electrode consistently lower than 20%. This interception current is higher than values previously reported [4], and could be reduced by increasing the aperture diameter though at the cost of having to increase the bias voltage, or by applying a larger bias voltage to the collector electrode.

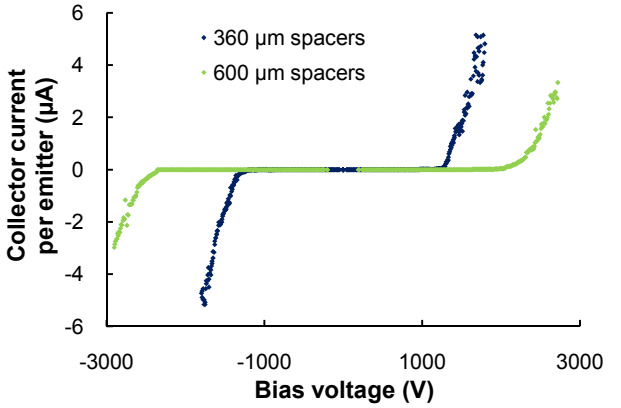

Figure 6: Per-emitter collector current vs. emitter-to-extractor bias voltage for a 7 by 7 emitter array, with 360 µm and 600 µm electrode spacing.

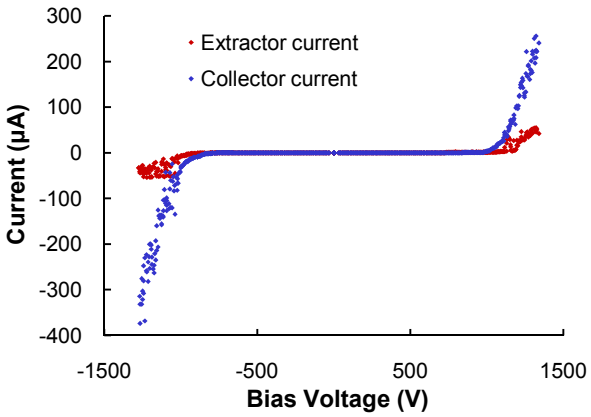

Figure 7: Extractor and collector current vs. emitter-to-extractor bias voltage for a 9 by 9 emitter array.

Current-voltage characteristics in the steady phase for all five emitter array sizes are shown in Fig. 8, using 360 µm thick spacers between the emitter and extractor electrodes in all cases. We obtained symmetric emission in both polarities with as much as 5 µA per emitter tip, five times higher than the best values previously reported in the literature [2]. Similar curve shapes and slopes indicate that the emitters operate uniformly in each of the different sized arrays. Lower start-up voltage was

observed for the 9 by 9 emitter array because the etched emitters were about 50 µm taller than in the other arrays.

Imprints (Fig. 9) on the collector electrode confirm that the emitters turn on uniformly across the arrays, with patterns on the collector plates that match the emitter array layouts. To calculate the beam divergence angle, the imprints from the 2 by 2 emitter array are used for reference. The imprint from a single emitter has a diameter of about 5.8 mm, and the collector is spaced 3.7 mm from the emitter tips, corresponding to a beam divergence semi-angle of 38°.

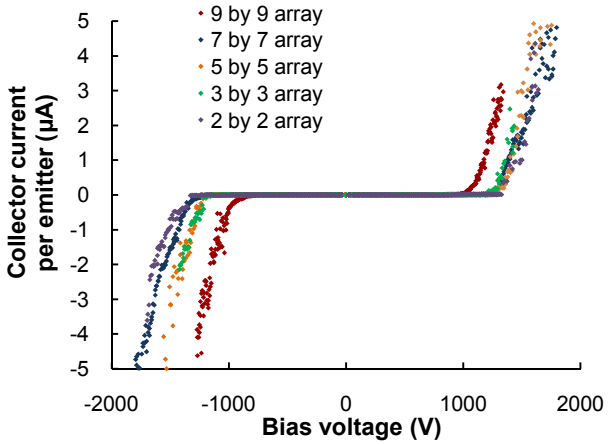

Figure 8: Per-emitter collector current vs. emitter-to-extractor bias voltage for five different emitter arrays.

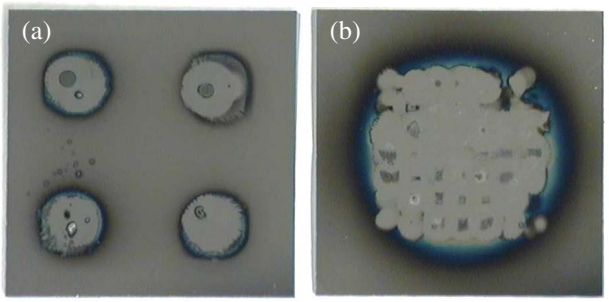

Figure 9: Electrospray imprints on the silicon collector electrode for (a) a 2 by 2 emitter array, (b) a 7 by 7 emitter array. Each silicon plate is 2 cm by 2 cm.

CONCLUSION

The first demonstration of a MEMS multiplexed electrospray source with integrated extractor grid and carbon nanotube (CNT) flow control structures for low-voltage high-throughput electrospray emission from ionic liquids in vacuum has been reported. The conformal carbon nanotube film grown on the surface of the emitters is a highly wetting coating that effectively transports the liquid to the emission sites at the emitter tips. Using devices containing 4, 9, 25, 49 and 81 emitters in 1 cm^2, symmetric emission in both polarities with as much as 5 µA per emitter tip was obtained – a factor of five higher than the best per-emitter values reported in the literature. Imprints on the collector electrode demonstrate uniform operation of the emitter arrays. Future work will include time-of-flight measurements to identify the distribution of ions and droplets in the spray generated by the electrospray source.

ACKNOWLEDGEMENTS

Microfabrication was completed using the facilities at the MIT Microsystems Technology Laboratories (MTL). This work was supported by the Defense Advance Research Projects Agency Microsystems Technology Office under contract W31P4Q-11-1-0007 (program manager J. Judy). Any opinions, findings, and conclusions or recommendations expressed in this publication are those of the authors and do not necessarily reflect the views of the US Government and therefore, no official endorsement of the US Government should be inferred.

REFERENCES

[1] R. Krpoun, K. L. Smith, J. P. Stark, H. R. Shea, "Tailoring the hydraulic impedance of out-of-plane micromachined electrospray sources with integrated electrodes," *Appl. Phys. Lett.,* vol. 94, 2009.

[2] R. S. Legge, P. C. Lozano, "Electrospray propulsion based on emitters microfabricated in porous metals," *J. Propul. Power,* vol. 27, pp. 485-494, 2011.

[3] L. F. Velásquez-García, A. I. Akinwande, M. Martínez–Sánchez, "A planar array of micro-fabricated electrospray emitters for thruster applications," *J. Microelectromech. S.,* vol. 15, pp. 1272-1280, 2006.

[4] B. Gassend, L. F. Velásquez-García, A. I. Akinwande, M. Martínez-Sánchez, "A microfabricated planar electrospray array ionic liquid ion source with integrated extractor," *J. Microelectromech. S.,* vol. 18, pp. 679-694, 2009.

[5] L. F. Velásquez-García, A. I. Akinwande, M. Martínez-Sánchez, "Precision hand assembly of MEMS subsystems using DRIE-patterned deflection spring structures: an example of an out-of-plane substrate assembly," *J. Microelectromech. S.,* vol. 16, pp. 598–612, 2007.

[6] B. Gassend, L. F. Velásquez-García, A. I. Akinwande, "Precision In-Plane Hand Assembly of Bulk-Microfabricated Components for High-Voltage MEMS Arrays Applications," *J. Microelectromech. S.,* vol. 18, pp. 332-346, 2009.

[7] P. D. Prewett, G. L. Mair, *Focused Ion Beams From Liquid Metal Ion Sources*. Hertfordshire, U.K.: Research Studies Press, 1991.

[8] I. Romero-Sanz, R. Bocanegra, J. Fernandez de la Mora, M. Gamero-Castano, "Source of heavy molecular ions based on Taylor cones of ionic liquids operating in the pure ion evaporation regime," *J. Appl. Phys.,* vol. 94, pp. 3599-3605, 2003.

[9] K. B. Teo, M. Chhowalla, G. A. J. Amaratunga, W. I. Milne, "Uniform patterned growth of carbon nanotubes without surface carbon," *Appl. Phys. Lett.,* vol. 79, pp. 1534-1536, 2001.

[10] P. Lozano, M. Martínez-Sánchez, "Ionic liquid ion sources: characterization of externally wetted emitters," *J. Colloid Interf. Sci.,* vol. 282, pp. 415-421, 2005.

CONTACT

*F.A. Hill, tel: +1-617-452-4903; fahill@mit.edu